J. of Chemical Physics

UCRL-19193
Preprint

c. 2

COLLISIONAL EXCITATION OF SMALL MOLECULAR IONS

M. H. Cheng, M. H. Chiang, E. A. Gislason,
B. H. Mahan, C. W. Tsao, and A. S. Werner

RECEIVED
LAWRENCE
RADIATION LABORATORY

MAR 23 1970

LIBRARY AND
DOCUMENTS SECTION

February 1970

AEC Contract No. W-7405-eng-48

TWO-WEEK LOAN COPY

This is a Library Circulating Copy which may be borrowed for two weeks. For a personal retention copy, call Tech. Info. Division, Ext. 5545

UCRL-19193

LAWRENCE RADIATION LABORATORY
UNIVERSITY of CALIFORNIA BERKELEY

34

DISCLAIMER

This document was prepared as an account of work sponsored by the United States Government. While this document is believed to contain correct information, neither the United States Government nor any agency thereof, nor the Regents of the University of California, nor any of their employees, makes any warranty, express or implied, or assumes any legal responsibility for the accuracy, completeness, or usefulness of any information, apparatus, product, or process disclosed, or represents that its use would not infringe privately owned rights. Reference herein to any specific commercial product, process, or service by its trade name, trademark, manufacturer, or otherwise, does not necessarily constitute or imply its endorsement, recommendation, or favoring by the United States Government or any agency thereof, or the Regents of the University of California. The views and opinions of authors expressed herein do not necessarily state or reflect those of the United States Government or any agency thereof or the Regents of the University of California.

Collisional Excitation of Small Molecular Ions

M. H. Cheng, M. H. Chiang, E. A. Gislason, B. H. Mahan, C. W. Tsao, and A. S. Werner

Department of Chemistry and Inorganic Materials Research Division of the Lawrence Radiation Laboratory, University of California, Berkeley 94720

We have determined velocity vector distributions for NO^+ and O_2^+ scattered from helium. As expected, the small angle scattering is elastic, but at angles greater than 60°, inelasticity which increases with the scattering angle is apparent. For angles greater than 100°, this inelasticity represents vibrational excitation of the molecule-ion. For initial relative kinetic energies between 4.3 and 26 eV and 180° scattering, the variation of the inelasticity is consistent with a new, corrected version of the classical theory of vibrational excitation. Three methods of calculating the angular variation of the inelasticity are presented and found to be consistent with the experimental data.

The collisional excitation of the vibrational and rotational motions of molecules is a problem of central importance in chemical kinetics, and has been the subject of a great many experimental and theoretical investigations. Several recent review articles and monographs[1-4] provide excellent summaries of the work which has been done. Virtually all theoretical analyses have dealt with one-dimensional models, and have given as their most direct result the probability of a vibrational transition, or the amount of energy transferred in a head-on collision of specified relative velocity. On the other hand, almost all experimental methods which have been used give a transition probability or energy transferred averaged over a Boltzmann distribution of velocities, and over all types of collision ranging from grazing to head-on. In contrast, ion beam experiments offer a more direct test of energy transfer theories, since one can determine the results of collisions between molecules whose relative energy can be well specified and varied over a wide range. Furthermore, by measuring the scattering angle one can differentiate between head-on and grazing collisions. Accordingly, in this paper we report our measurements of the velocity vector distributions of NO^+ and O_2^+ scattered by helium, and analyze them in terms of certain of the simple theories of vibrational excitation.

EXPERIMENTAL

The apparatus used in this work has been described in detail in an earlier publication.[5] It consists of a magnetic

mass spectrometer for preparation of the primary ion beam of known energy, a scattering cell containing the target gas, a 90° spherical electrostatic energy analyzer, a quadrupole mass spectrometer, and an ion counter. The energy distributions of ions scattered through various laboratory angles were determined by sweeping the electrostatic energy analyzer, and the angular distribution of ions of fixed energy was measured by rotating the entire detection train with respect to the primary ion beam. After normalization of the ion intensities to unit primary beam current, scattering gas density, scattering volume, and velocity space volume intercepted by the detector, contour maps of the normalized scattered intensity per unit velocity space volume are constructed. In all respects the details of the data acquisition and treatment are the same as those employed in our previous publications.

The primary ions were produced by microwave discharge of the parent gases. Beam attenuation experiments of the type described by Turner et al[6] showed that the mass-analyzed beams contained less than 3% metastable electronically excited ions. The extent of the vibrational excitation of the primary ions is not known, but Franck-Condon factors[7] suggest that the ions are principally in the lowest three or four vibrational states.

RESULTS

Eighteen experiments were performed on the NO^+-He system, and at five initial energies enough data were taken to allow construction of complete contour maps of the scattered ion

intensity. For the O_2^+-He system, contour maps were made for three initial energies. In other experiments, a profile of the scattered intensity along the initial relative velocity vector (the 0°-180° line in the barycentric system) was made.

Figure 1 shows an intensity contour map which exemplifies the data taken for the NO^+-He system, and Fig. 2 shows a similar map of the intensity of O_2^+ scattered by helium. The quantity Q given in these maps is the difference between the final and initial relative energies of the collision partners. Thus the locus of elastically scattered ions is given in each map by the large circle labelled Q = 0. In both maps it is clear that the small angle scattering is most intense, and very nearly elastic, as expected. At larger scattering angles, the intensity maxima fall at velocities which correspond to negative Q; that is, to inelastic scattering. As the scattering angle increases, the Q values at the intensity maxima become increasingly negative. These qualitative features were found in all of the contour maps determined in our work.

The experiment represented in Fig. 2 was conducted at a relative energy of 11.1 eV, which considerably exceeds 6.8 eV, the dissociation energy of O_2^+. The intensity maxima lie at Q values considerably more positive than -6.8 eV, which clearly demonstrates that dissociative collisions are comparatively rare, even when the relative energy of collision is much greater than the bond dissociation energy. Direct measurement of the fragment ion intensity, which we report in another publication, confirms the small cross section for dissociative

collisions. However, in Fig. 2 there is an intensity contour which falls inside the Q = -6.8 eV circle, where O_2^+ should not be observed, because of its instability with respect to dissociation. As we have pointed out in previous publications,[5] this apparent scattering into regions forbidden by product stability or energy conservation conditions is a consequence of the finite energy and angular resolution of the apparatus, and of the motion of the target gas molecules.

In order to remove the effects of apparatus resolution, we have deconvoluted the intensity profiles of the O_2^+ scattered through 180°. This was accomplished with a numerical iterative smoothing-deconvolution program similar to those described in Ioup and Thomas,[8] and Morrison.[9] The results are shown in Fig. 3. It is important to notice that the position of the intensity maximum is unchanged by the deconvolution. However, the intensity profile is narrowed and virtually all the scattering in the forbidden region is removed by the deconvolution. If the effect of the motion of the target molecules were taken into account, the intensity profile would be further narrowed, but would not be shifted in position, since the motion of the target gas molecules is isotropic, and the scattering cross section is not a sensitive function of relative velocity. Consequently, we can interpret the positions of the intensity maxima in the primary data as correctly representing the magnitude of the most probable energy loss.

DISCUSSION

At the relatively high energies employed in these experiments, the deBroglie wavelength associated with relative motion is much smaller than the characteristic distances of the interaction potential and the vibrational amplitudes. The Q values indicate that changes of 10 or more in the vibrational quantum number occur, and of course excitation to individual states is not resolved. Thus it seems most appropriate to discuss the experimental results in the framework of classical vibrational energy transfer theory.

Since the relative velocities v_o were approximately 3×10^6 cm/sec, and the characteristic length L of the exponential potential used in disucssing vibrational energy transfer is approximately 2×10^{-9} cm, the dimensionless parameter $\omega L/v_o$ is less than 0.3 for the vibrational frequencies ω of the molecules used in these experiments. Consequently, the collisions occur under near-impulse conditions, and it is not unreasonable to compare the experimental results with the predictions of an impulse or billiard-ball model. In this model, a particle A (the helium atom) is assumed to be initially stationary, and to collide elastically with particle B of the BC projectile, while the particle C moves with its original velocity throughout the collision. A velocity vector diagram representing this process is shown in Fig. 4. The velocity of the BC center-of-mass after the collision can be found by elementary vector addition, nad from this the following

expression for the energy ΔE transferred to internal modes of BC can be derived:

$$\Delta E/E_r = 2[m^{-1} + \sin^2\theta - \cos\theta(m^{-2} - \sin^2\theta)^{1/2}]/(1 + m^{-1})^2 \quad (1)$$

Here E_r is the initial relative energy of the collision, θ is the center-of-mass scattering angle, and the parameter m is given by

$$m = M_A M_C/(M_B)(M_A + M_B + M_C)$$

For head-on collisions between A and B which produce scattering to $\theta = 180°$, we have

$$\Delta E/E_r = 4\, M_A M_B M_C (M_A + M_B + M_C)/(M_A + M_B)^2 (M_B + M_C)^2 \quad (2)$$

For an O_2^+-He head-on collision, $\Delta E/E_r$ should be 0.3600, independent of energy, while for the NO^+-He system, $\Delta E/E_r$ is 0.3385 and 0.4124 when particle B is oxygen and nitrogen respectively, which gives an average of 0.3754.

Another simple model[4] with which our data can be compared is the classical harmonic oscillator which is "driven" by a time dependent force arising from the collision. For a repulsive exponential interaction between atoms A and B, the conventional solution to this problem is

$$\Delta E/E_r = 4(M_B M_C/M_B M)(\pi\omega L/v_o)^2 \operatorname{csch}^2 (\pi\omega L/v_o) \quad (3)$$

where M is equal to the sum of all masses. Kelley and Wolfsberg[10] and Rapp and Kassal[4] have noted that this expression behaves incorrectly in the high velocity limit, in that it predicts

excitations in excess of the total relative energy of collision. The source of the difficulty[11] lies in the assumption made in the derivation that the potential energy at the turning point in the collision is equal to the initial energy of A relative to the entire BC molecule. In fact, the derivation represents a refinement of the impulse approximation, and so the appropriate value for the energy at the turning point is the initial energy of A relative to the B atom alone. When this correction is made, the result is

$$\Delta E/E_r = [4M_A M_B M_C M/(M_A+M_B)^2(M_B+M_C)^2](\pi\omega L/v_o)^2 \operatorname{csch}^2(\pi\omega L/v_o) \quad (4)$$

This expression converges properly to the impulse approximation at the high velocity limit, and over much of the velocity range is in close agreement with the results of exact computer integration[10] of the equations of motion.

In Figs. 5 and 6 we compare the predictions of the various versions of the classical vibrational excitation theory with experimental data for the excitation energy occurring in collisions in which the scattering angle was 180°. These head-on collisions necessarily involve only small amounts of angular momentum associated with the orbital motion of the collision partners, and thus the excitation energy is very probably mostly in the form of molecular vibration rather than rotation. Consequently, these data should be most comparable to the theories which, with the exception of the impulse model, are one-dimensional.

We see from Figs. 5 and 6 that the predictions of the impulse model exceed the measured inelasticities by substantial amounts. This is not particularly surprising, since for the primitive impulse approximation to be accurate we must have $\omega L/v_o << 1$, while in fact the parameter is greater than 0.1 even at the highest energies. It seems likely that impulse conditions can be reached at velocities where the collision is electronically adiabatic only if the vibration frequency of the molecule is much less than 1000 cm^{-1}.

The predictions of the conventional version of classical vibrational excitation theory, Eq. (3), are in poor agreement with both the exact results and experimental data, and actually exceed the impulse approximation at high energies. In contrast, the corrected version of the theory, Eq. (4), is in very good agreement with experiment and with the "exact" results obtained by applying the correction factor of Rapp and Kassal[4] to Eq. (3). For both Figs. 5 and 6 we have used values of L in the theoretical expressions, derived from Herzfeld's[12] relation $L = r_o/17.5$, where r_o is the average of the Lennard-Jones distance parameters for He and NO or O_2. The predictions of the theories are not at all sensitive to the value chosen for L, particularly at the higher energies. When L for the NO^+-He ststem was taken to be 0.1632 and 0.1840, the calculated excitation energies differed from the ones given in Fig. 5 by less than 10% at relative energies above 4 eV, and less than 3% above 14 eV. It appears, therefore, that the amount of energy transferred into vibration at these

higher energies is principally determined by the masses of the atoms, and to a lesser degree by the group $\omega L/v_o$. Consequently, Eq. (4) may be used with some confidence to predict the inelasticity of head-on collisions at high energy.

It is likely that simultaneous vibrational and rotational transitions are responsible for the inelastic scattering which falls at angles appreciably smaller than 180°. Nevertheless, it is of interest to see how the predictions of the approximate classical theories of vibrational excitation compare with measured inelasticities at all scattering angles. While the simple classical theory of vibrational excitation is one-dimensional, it can be extended to three dimensions by the modified wave number approximation (MWNA) of Takayanagi.[1] For a classical situation, the consequences of this approximation may be derived as follows. If the total energy associated with orbital motion is conserved, the kinetic energy associated with radial motion in a spherical potential V(r) is

$$\frac{1}{2}\mu' \dot{r}^2 = E - V - E(b/r)^2 \tag{5}$$

and the impact parameter and turning point r_c are related by

$$(b/r_m)^2 = 1 - V(r_m)/E \tag{6}$$

Here μ' is the reduced mass of the collision pair, b is the impact parameter, E is the total energy, and $V(r_m)$ is the potential energy at the turning point. In making the modified wave number approximation, it is assumed that in the last term of Eq. (5) the variable r can be replaced by its value r_m at the turning point. Thus substituting Eq. (6) into Eq. (5), we

get

$$\frac{1}{2}\mu'\dot{r}^2 = V(r_m) - V \tag{7}$$

which is the energy conservation equation for a particle with total energy $V(r_m)$ moving in one dimension. Thus the MWNA consists of reducing the three dimensional problem to one-dimensional motion in which the total energy or initial relative kinetic energy is equal to the potential energy at the turning point in the three-dimensional problem. Since the excitation energy can be calculated from the initial kinetic energy, the angular dependence of the inelasticity can be calculated if the scattering angle is known as a function of E and $V(r_m)$. For simplicity, we select the hard sphere interaction for which the potential energy at the turning point can be taken equal to the radial kinetic energy at the instant of impact, E_{rad}. This quantity is related to the initial energy and the scattering angle θ by

$$E_{rad} = E \sin^2(\theta/2) = V(r_m) \tag{8}$$

or

$$v_{rad} = v_o \sin(\theta/2) \tag{9}$$

Thus in order to calculate the inelasticity at an angle θ, the radial velocity v_{rad} is found from Eq. (9) and used in Eq. (4) to compute ΔE.

The use of hard-sphere scattering angles in this calculation may seem unrealistic, but in fact is a fairly good approximation for scattering near 180° at high energies.[13] In any case, the great simplicity of this procedure makes it worth testing against experimental data. Later we shall

improve upon this primitive MWNA by using the exact deflection angles for the exponential potential.

In Fig. 7 we compare the inelasticity calculated by the primitive MWNA, and by the impulse approximation Eq. (1), with experimental results. It is clear that the impulse approximation overestimates the inelasticity at all angles greater than 90°, where the experimental values are particularly reliable. The results of the 180° scattering discussed earlier might have caused us to anticipate this discrepancy.

The apparent success of the primitive MWNA in predicting the angular distribution of vibrational inelasticity raises the question of the importance of rotational inelasticity. The present application of the MWNA contains no provision for rotational inelasticity, and if this is an important factor, the agreement between experiment and MWNA is purely fortuitous. To resolve this question, it is necessary to determine the maximum impact parameters and orbital angular momenta which are involved in collisions which give scattering to approximately 100° in the barycentric system. Accordingly, we have computed exact scattering angles for the exponential repulsive potential $V_o \exp(-r/L)$.

For values of the parameters V_o and L which are appropriate for the NO^+-He and O_2^+-He systems, an impact parameter of approximately 0.7 A gives scattering to 100°. For the 6.55 eV NO^+-He experiment, the orbital angular momentum for this angle is therefore approximately 75 $\hbar$, if the initial velocity is 1.9×10^6 cm/sec. The fraction of this orbital angular momentum

which is converted to rotation of the target is not limited by the conservation laws, and is consequently difficult to estimate. If the ion-molecule potential were so anisotropic that all the orbital rotation were converted to rotation of the molecule, the final rotational energy of the molecule would be approximately 0.9 eV, which is greater than the observed inelasticities at scattering angles of 100° in the 6.55 eV experiment. On the other hand, it seems unlikely that the molecular ion-atom potential is sufficiently anisotropic to induce such an angular momentum change, except at the highest collision energies. As a very rough estimate of the anisotropy we can take the ratio of the internuclear distance in NO^+ or O_2^+ to the Lennard-Jones σ parameter for the NO^+-He or O_2^+-He pair. These ratios are approximately 0.4. If this fraction of the orbital angular momentum is converted to molecular rotation, the corresponding inelasticity would be 0.14 eV, which is just less than the experimental uncertainty in the measured inelasticity. Thus it is quite possible that rotational inelasticity is not important at angles as small as 100°. A much stronger statement can be made for scattering angles of 120° or greater. These correspond to impact parameters of 0.5 A or less, orbital angular momenta no greater than approximately 55, and rotational inelasticities which are probably less than 0.1 eV. Thus the inelasticity at these larger scattering angles is principally due to excitation of vibration, and the fact that the primitive MWNA is in agreement with the experimental results is an indication of the usefulness of

this procedure for estimating vibrational inelasticities.

It is possible to use a slightly more refined version of the MWNA if the exact deflection angle is known as a function of the potential energy at the turning point or distance of closest approach in the collision. In Table 1 the results of this refined MWNA are compared with the predictions of the primitive version (PMWNA) in which hard-sphere scattering angles are used. The similarity between the two results shows that the primitive MWNA can be used with some confidence in this large angle, high energy regime.

There is still another approximate method of estimating the energy transfered to vibration when the impact parameter is nonzero. In this approach we again assume that the molecule is represented by a breathing sphere, and that the inelasticity of the collision is determined only by the characteristics of the radial motion near the turning point of the orbit. We also assume that over the significant range of r, the effective intermolecular force is a constant equal to the effective force at the turning point. Thus for the separation r between the centers of force we write

$$r - r_m = \frac{1}{2}\ddot{r}t^2 \tag{10}$$

where t is zero at the turning point r_m, and $\ddot{r}$ is given by

$$\ddot{r} = -(1/\tilde{m})(\partial V_{eff}/\partial r)_{r=r_m} \tag{11}$$

As a consequence of Eq. (10), we refer to this treatment as the parabolic trajectory approximation, or PTA. In Eq. (11),

the quantity $\tilde{m}$ is a reduced mass, which may be taken as that of the two colliding atoms, if the collisions approximately satisfy the conditions for the impulse limit. The effective potential V_{eff} is given by

$$V_{eff} = V + E(b^2/r^2)$$

where V is the true potential energy, b is the impact parameter, and E is the initial relative kinetic energy of the two atoms which collide. Consequently,

$$2a \equiv (\ddot{r})_{r_m} = \tilde{m}^{-1}[F(r_m) + 2E(b^2/r_m^3)]$$

where F is the force.

If we choose a potential of the form

$$V = V_o \exp(-r/L)$$

then the time dependent force which drives the oscillator is

$$F(t) = (\gamma V_m/L) \exp(-at^2/L)$$

Here γ is the mass ratio $M_C/(M_B + M_C)$, where atom B of the diatomic molecule BC is in collision with atom A. The energy ΔE transferred to an initially nonvibrating oscillator of reduced mass μ and frequency ω is given by

$$\Delta E = (2\mu)^{-1} [\int_{-\infty}^{\infty} F(t) \cos\omega t \, dt]^2$$

and consequently for the PTA we get

$$\Delta E \doteq (2\mu)^{-1}(\gamma V_m/L)^2(\pi L/a)\exp(-L\omega^2/2a) \qquad (12)$$

For head-on collisions in the high velocity limit, this expression gives a result which is $\pi/4$ times the true impulse limit, since the PTA gives a time dependent force which varies too

slowly near t = 0 for such collisions. For grazing collisions, however, the PTA gives a result in the limit of infinite impact parameter which is identical to the answer obtained from a classical straight line trajectory treatment.[11] Consequently, it would appear that use of the MWNA at very large angles, and the PTA at smaller angles would give the most accurate predictions of the inelasticities.

Table I contains the inelasticities at 5 angles calculated by means of PTA, PMWNA, and MWNA for two exponential potentials, along with the experimentally determined results. The potential

$$V = 6550 \exp(-r/0.7146) \qquad (\text{eV-Å})$$

was chosen rather arbitrarily, since no previously determined potentials exist for the energies employed in these experiments. The potential with the smaller pre-exponential factor was chosen to provide contrast. A perusal of Table 1 shows that the results calculated for the two potentials by the same method do not differ appreciably except at the smallest angle. This result is not too surprising, since it has long been known that the pre-exponential factor does not affect the energy transferred in a head-on collision at all. It appears that if vibrational inelasticity is ever to be used to determine the pre-exponential part of intermolecular potentials, accurate measurements of the inelasticity at angles near 90° must be made.

Aside from the fact that the PTA underestimates the inelasticity at 180°, the three methods of calculating the

inelasticity give similar results. None of the three methods quite reproduces the rapidity of the decrease in inelasticity with decreasing angle, but the error is not large, and seldom greatly exceeds the ±0.15 eV uncertainty in the experimental data. It appears that until data of better quality at smaller angles become available and provide a more critical test, the primitive modified wave number method provide the best combination of accuracy and convenience for the prediction of vibrational inelasticities.

Acknowledgement: This work was supported by the U. S. Atomic Energy Commission. E.A.G. wishes to acknowledge a postdoctoral fellowship from the National Center for Air Pollution Control of the Public Health Service.

Table I. Experimental and Calculated Vibrational Inelasticities for NO^+-He Collisions.[a]

E_{rel}	V=6550 exp(-r/0.1746				EXP	V=655 exp(-r/0.1746)	
	θ	PTA	PMWNA	MWNA		PTA	MWNA
4.30	180	0.90	0.85	0.85	1.0	0.90	0.85
	160	0.87	0.82	0.80	1.0	0.86	0.80
	140	0.77	0.75	0.70	0.88	0.77	0.70
	120	0.64	0.65	0.55	0.64	0.63	0.57
	100	0.48	0.52	0.45	0.52	0.47	0.43
6.55	180	1.39	1.50	1.50	1.3	1.39	1.50
	160	1.35	1.40	1.45	1.5	1.36	1.48
	140	1.22	1.25	1.30	1.1	1.23	1.35
	120	1.02	1.00	1.15	0.81	1.02	1.13
	100	0.79	0.70	0.85	0.65	0.85	0.95
8.85	180	2.04	2.30	2.3	2.4	2.04	2.30
	160	1.97	2.20	2.2	2.1	1.99	2.25
	140	1.77	1.95	2.0	--	1.78	2.05
	120	1.48	1.50	1.7	1.50	1.56	1.85
	100	1.12	1.10	1.3	1.42	1.17	1.40
10.7	180	2.57	3.0	3.0	2.8	2.57	3.0
	160	2.48	2.9	2.9	2.9	2.51	2.90
	140	2.30	2.5	2.7	2.3	2.36	2.75
	120	1.94	2.0	2.3	1.8	1.91	2.35
	100	1.46	1.4	1.8	--	1.57	2.00
12.9	180	3.23	3.75	3.75	3.3	3.23	3.75
	160	3.11	3.65	3.70	2.9	3.15	3.70
	140	2.87	3.30	3.45	2.9	2.91	3.55
	120	2.40	2.75	2.95	2.3	2.35	2.95
	100	1.97	1.85	2.45	--	1.90	2.48

a. All energies in eV. PTA; parabolic trajectory approximation; PMWNA, primitive modified wave number approximation; MWNA, modified wave number approximation; EXP, experiment.

References

1. K. Takayanagi, Prog. Theoret. Phys. Supp. (Japan) **25**, 1 (1963).
2. K. Takayanagi, Advan. At. Mol. Phys. **1**, 149 (1965).
3. T. L. Cottrell and J. C. McCoubrey, Molecular Energy Transfer in Gases (Butterworth's Ltd., London, 1961).
4. D. Rapp and T. Kassal, Chem. Rev. **69**, 61 (1969).
5. W. R. Gentry, E. A. Gislason, B. H. Mahan, and C. W. Tsao, J. Chem. Phys. **49**, 3059 (1968).
6. B. Turner, J. Rutherford, and D. M. Compton, J. Chem. Phys. **48**, 1602 (1968).
7. R. W. Nichols, J. Physics B, **1**, 1192 (1968).
8. G. Ioup and B. Thomas, J. Chem. Phys. **46**, 3959 (1967).
9. J. D. Morrison, J. Chem. Phys. **39**, 200 (1963).
10. J. D. Kelley and M. Wolfsberg, J. Chem. Phys. **44**, 324 (1966).
11. B. H. Mahan, J. Chem. Phys. (to be published).
12. K. Herzfeld and T. A. Litovitz, Absorption and Dispersion of Ultrasonic Waves (Academic Press, Inc., New York, 1959).
13. E. M. Baroody, Phys. Fluids **5**, 925 (1962).

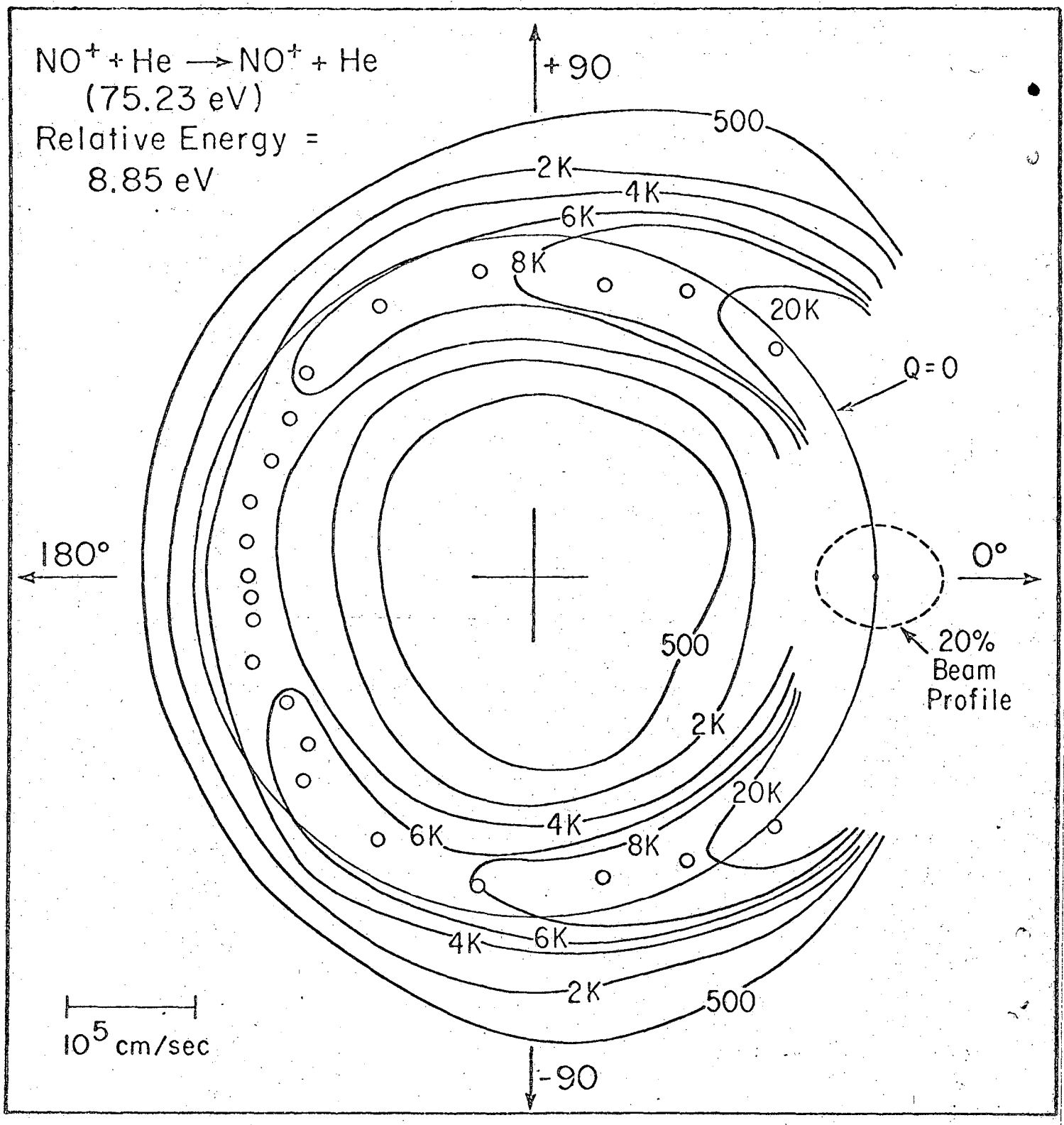
$NO^+ + He \rightarrow NO^+ + He$
(75.23 eV)
Relative Energy =
8.85 eV
+90
-90
180°
0°
500
2K
4K
6K
8K
20K
Q=0
20%
Beam
Profile
10^5 cm/sec

Fig. 1

Fig. 1. A contour map of the specific intensity of NO^+ scattered from He plotted as a function of the velocity in the center-of-mass coordinate system. The circle labelled Q = 0 is the locus of elastically scattered NO^+. The small circles locate the intensity maxima found in scans of the energy and angular distribution.

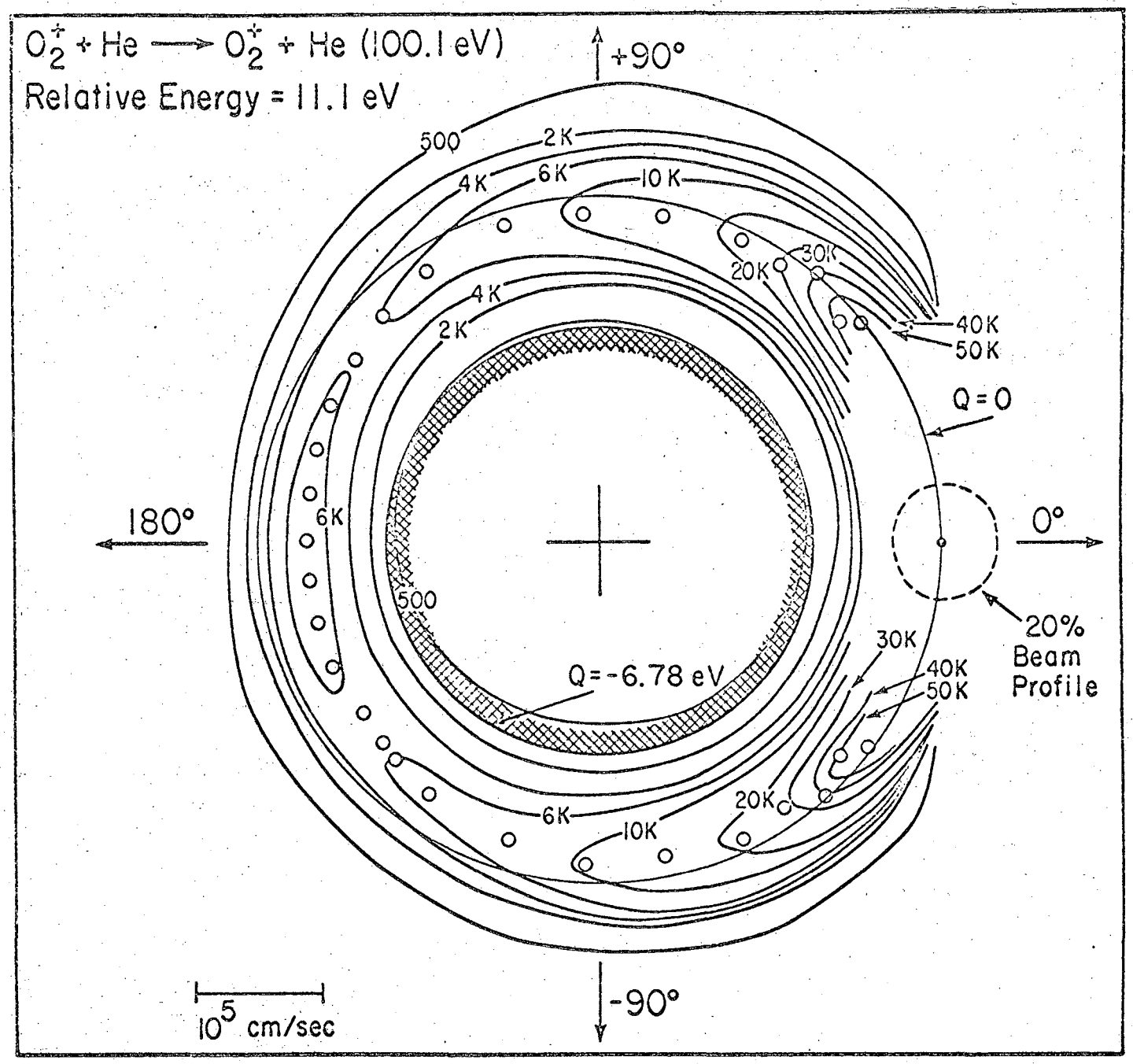
$O_2^+ + He \longrightarrow O_2^+ + He$ (100.1 eV)
Relative Energy = 11.1 eV
+90°
-90°
180°
0°
500
2K
4K
6K
10K
20K
30K
40K
50K
Q = 0
Q = -6.78 eV
20% Beam Profile
10^5 cm/sec

Fig. 2

Fig. 2. A contour map of the specific intensity of O_2^+ scattered from He plotted as a function of the velocity in the center-of-mass coordinate system. The circle labelled Q = 0 is the locus of elastically scattered O_2^+. The circle labelled Q = -6.8 surrounds a region of velocity space which is forbidden because of the instability of O_2^+ with respect to dissociation. The small circles locate the intensity maxima found in scans of the energy and angular distribution.

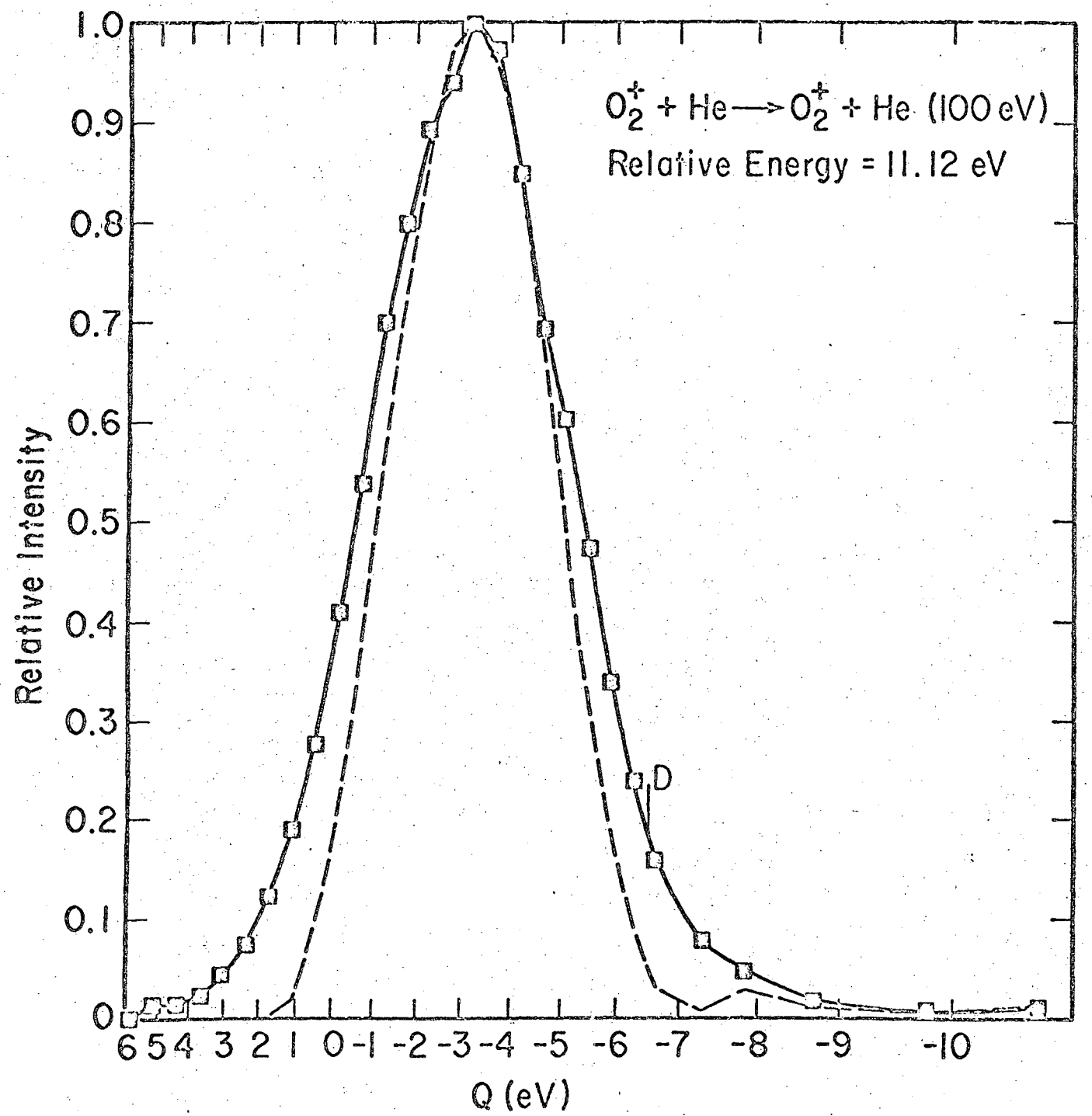
$O_2^+ + He \longrightarrow O_2^+ + He$ (100 eV)
Relative Energy = 11.12 eV
Relative Intensity
1.0
0.9
0.8
0.7
0.6
0.5
0.4
0.3
0.2
0.1
0
D
6 5 4 3 2 1 0 -1 -2 -3 -4 -5 -6 -7 -8 -9 -10
Q (eV)

Fig. 3

Fig. 3. A comparison of the measured intensity distribution of O_2^+ scattered through 180° in the center-of-mass system (solid line), and the same distribution after smoothing and deconvolution (dashed line) using the measured primary beam distribution as the apparatus resolution function. Note that the deconvolution removes most of the intensity which occurs in the "forbidden" region where $Q < D = -6.8$ eV. Also note that the smoothing-deconvolution introduces small subsidiary intensity maxima which have no obvious physical cause, and must be attributed to non-random experimental error.

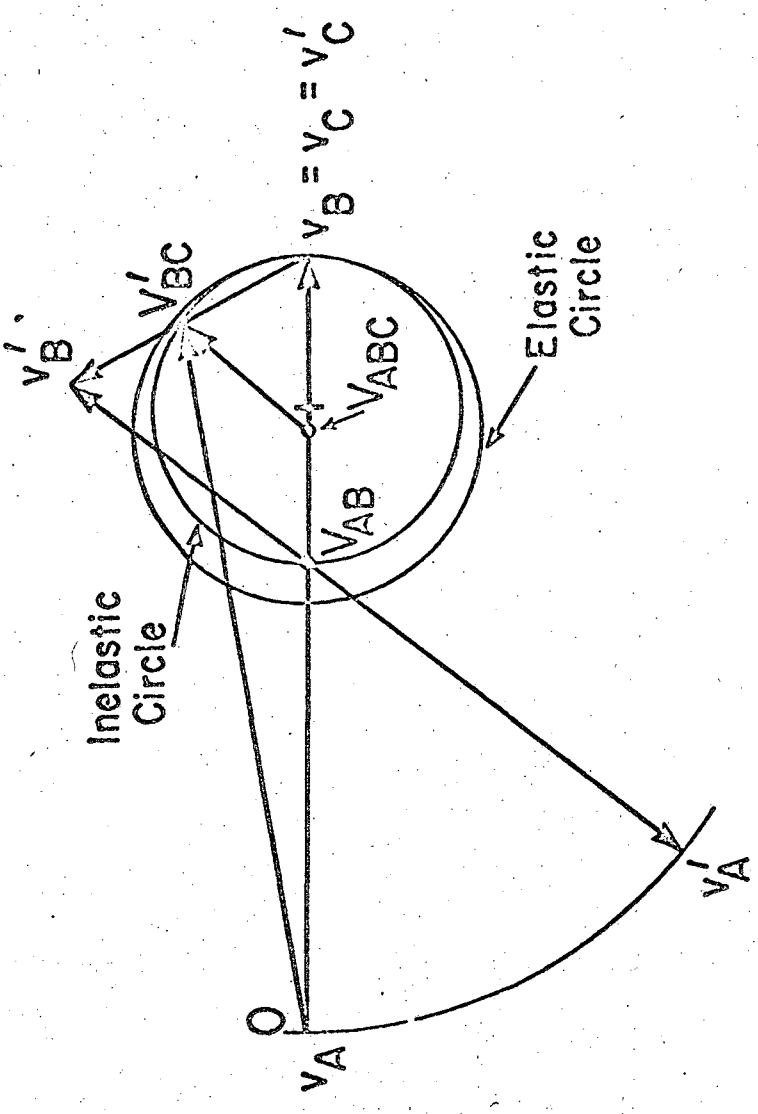
$v_B = v_C = v'_C$
v'_{BC}
v'_B
v_{ABC}
Elastic Circle
v_{AB}
Inelastic Circle
O
v_A
v'_A

Fig. 4

Fig. 4. Velocity vector diagram for the hard-sphere collision the stationary target atom A with the B atom of the BC projectile. The symbols v_B, v_B' denote respectively the initial and final velocities of B, and similar notation applies to the other velocities. V_{AB} refers to the velocity of the center of mass of the AB system. The elastic circle has as its center the center of mass velocity of the system V_{ABC}. The inelastic circle is centered on the cross half way between V_{AB} and v_B.

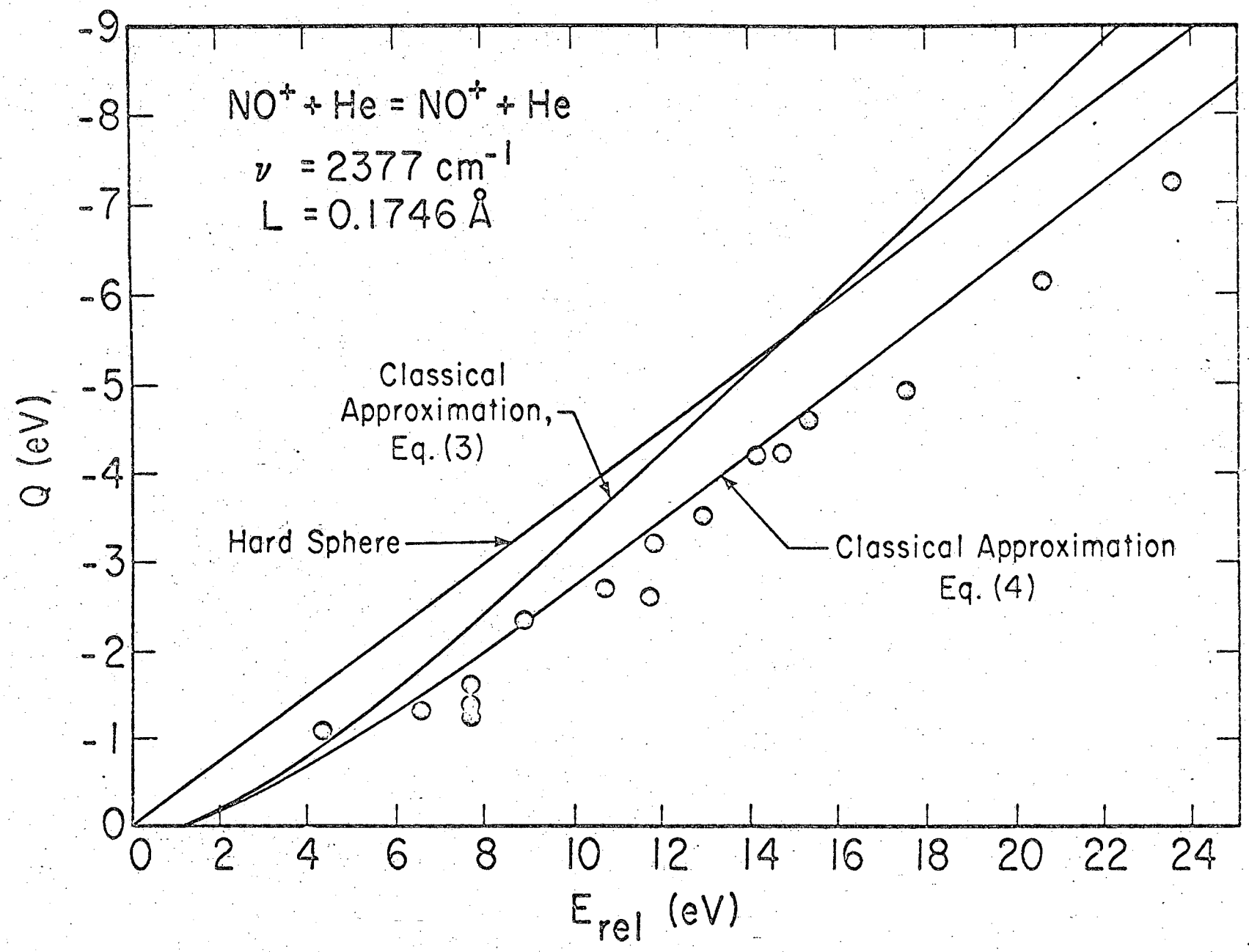
$NO^+ + He = NO^+ + He$
ν = 2377 cm^{-1}
L = 0.1746 Å
Classical Approximation, Eq. (3)
Hard Sphere
Classical Approximation Eq. (4)
Q (eV)
E_{rel} (eV)
-9
-8
-7
-6
-5
-4
-3
-2
-1
0
0
2
4
6
8
10
12
14
16
18
20
22
24

Fig. 5

Fig. 5. A plot of the experimental and theoretical Q values for 180° scattering of NO^+ by He as a function of initial relative energy. The closed circles represent the experimentally measured most probable Q values. The hard sphere approximation fails at all energies, the conventional classical approximation fails at high energies, while the refined impulse approximation is reasonably accurate at all energies.

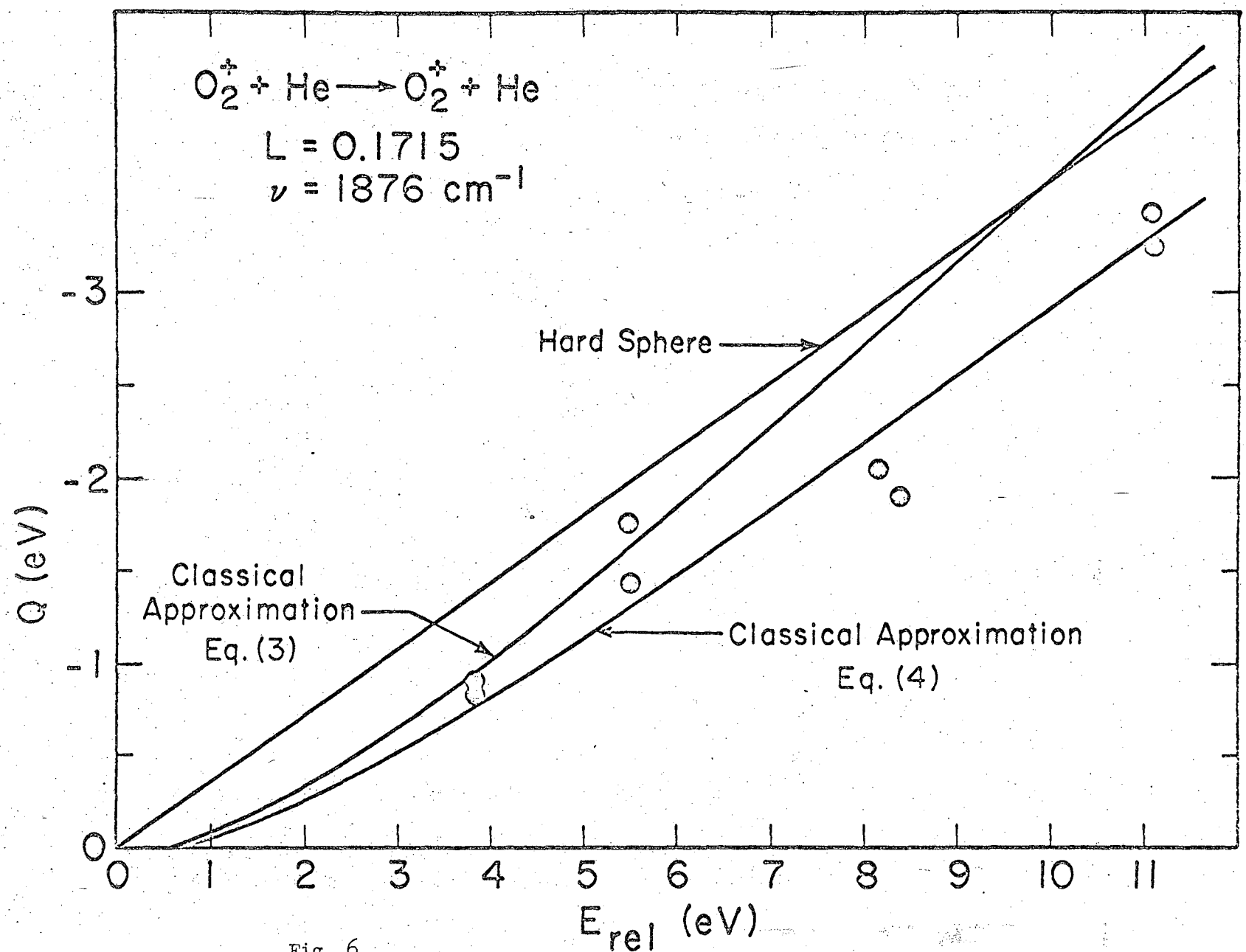
$O_2^+ + He \longrightarrow O_2^+ + He$
L = 0.1715
ν = 1876 cm^{-1}
Hard Sphere
Classical Approximation Eq. (3)
Classical Approximation Eq. (4)
Q (eV)
E_{rel} (eV)
0
-1
-2
-3
0
1
2
3
4
5
6
7
8
9
10
11

Fig. 6

Fig. 6. A plot of the experimental and theoretical Q values for 180° scattering of O_2^+ by He as a function of initial relative energy. The closed circles represent the experimentally measured most probable Q values. The hard sphere approximation fails at all energies, the conventional classical approximation fails at high energies, while the refined impulse approximation is reasonably accurate at all energies.

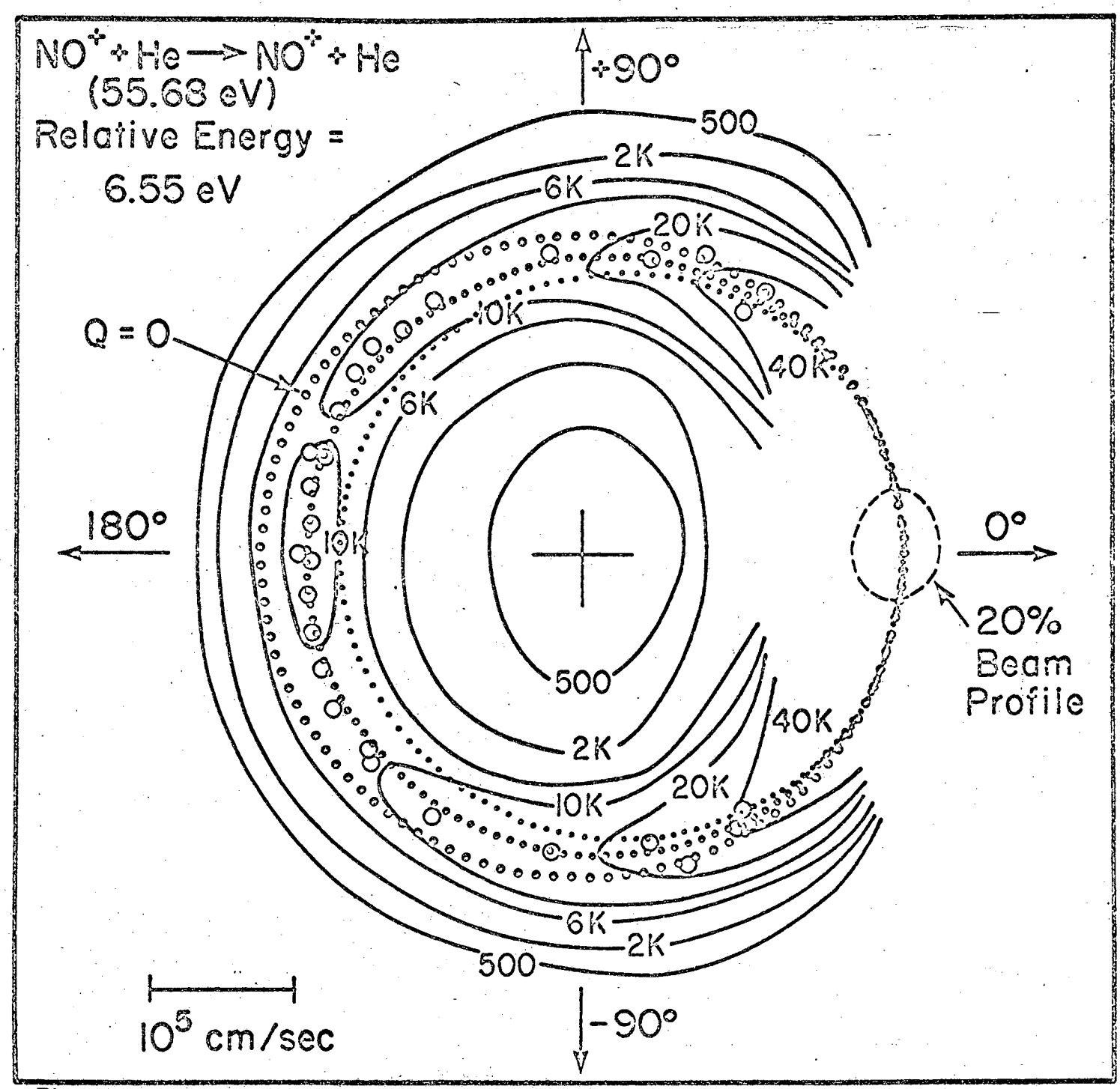
$NO^+ + He \rightarrow NO^+ + He$
(55.68 eV)
Relative Energy =
6.55 eV
+90°
-90°
180°
0°
Q = 0
500
2K
6K
20K
10K
40K
20%
Beam
Profile
10^5 cm/sec

Fig. 7

Fig. 7. A contour map of the specific intensity of NO^+ scattered from He plotted as a function of the velocity in the center-of-mass coordinate system. The small open circles give the locations of the intensity maxima determined experimentally. The largest closed dots give the locus of elastically scattered NO^+, the smallest closed dots give the locus of inelastically scattered NO^+ as predicted by the hard sphere impulse model, and the intermediate sized dots represent the predictions of the primitive modified wave number method.

LEGAL NOTICE

This report was prepared as an account of Government sponsored work. Neither the United States, nor the Commission, nor any person acting on behalf of the Commission:

A. Makes any warranty or representation, expressed or implied, with respect to the accuracy, completeness, or usefulness of the information contained in this report, or that the use of any information, apparatus, method, or process disclosed in this report may not infringe privately owned rights; or

B. Assumes any liabilities with respect to the use of, or for damages resulting from the use of any information, apparatus, method, or process disclosed in this report.

As used in the above, "person acting on behalf of the Commission" includes any employee or contractor of the Commission, or employee of such contractor, to the extent that such employee or contractor of the Commission, or employee of such contractor prepares, disseminates, or provides access to, any information pursuant to his employment or contract with the Commission, or his employment with such contractor.

TECHNICAL INFORMATION DIVISION
LAWRENCE RADIATION LABORATORY
UNIVERSITY OF CALIFORNIA
BERKELEY, CALIFORNIA 94720